Available online at www.sciencedirect.com
ScienceDirect
Journal of Organometallic Chemistry 692 (2007) 2508–2518
Journal of Organometallic Chemistry
www.elsevier.com/locate/jorganchem

Persistent π-arene interactions in bulky formamidinate complexes of potassium

Marcus L. Cole [a,b], Aaron J. Davies [a,c], Cameron Jones [a], Peter C. Junk [a,*]

[a] School of Chemistry, Monash University, Vic. 3800, Australia
[b] School of Chemistry and Physics, University of Adelaide, Adelaide, SA 5005, Australia
[c] School of Chemistry, Main Building, Cardiff University, Cardiff CF10 3AT, UK

Received 8 January 2007; received in revised form 18 February 2007; accepted 20 February 2007
Available online 24 February 2007

Abstract

The reaction of potassium hexamethyldisilazide (K-HMDS) with 1 equiv. of the bulky formamidine N(Diep)=C(H)NH(Diep) (DiepFormH, Diep = 2,6-$Et_2C_6H_3$) in THF yields the half deprotonated compound [K(DiepForm)(DiepFormH)] (**1**), which exhibits suppressed reactivity with the hexamethyldisilazide anion. Reaction of **1** with *n*-BuLi gives the polymer $[\{Li(THF)_2K(DiepForm)_2\}_n]$ (**2**). Preparation of **1** in the presence of the chelating solvents 1,2-dimethoxyethane (DME) or *N*,*N*,*N*′,*N*″,*N*″-pentamethyldiethylenetriamine (PMDETA) gives the fully deprotonated species $[\{K_3(DiepForm)_3(DME)_3\}_n]$ (**3**) and [{K(PMDETA)K(DiepForm)$_2$}$_n$] (**6**). The syntheses of compounds **1**–**3**, **6** and related compounds, e.g. $[\{K_3\{N(Dimp)C(H)N(Dimp)\}_3(DME)_3\}_n]$ (**4**) (Dimp = 2,6-$Me_2C_6H_3$), are described.

Keywords: Alkali metals; Potassium; Amides; Amidinates; Molecular structures

1. Introduction

In recent years the *N*,*N*′-bis(aryl)formamidinate ligand (Fig. 1) has demonstrated an unrivalled coordinative flexibility within the amidinate family of organoamide support ligands [1]. Variants possessing bulky *N*-substituents, e.g. 2,6-diisopropylphenyl (Dipp), have found great utility in alkaline earth [2], lanthanoid [3] and group 13 chemistry [4] not-least because of their ability to support mononuclear, dinuclear and higher nuclearity species using a variety of binding modes. This facet of their chemistry is permitted by flexibility about the NC(H)N central methine group, which can open and close to correspond with the metal assembly at hand [5].

In 2002 we reported the first example of a new type of *N*,*N*′-bis(aryl)amidinate binding mode (Fig. 1) which necessitates a *Z-anti* [6] amidinate that chelates using a single amido nitrogen and π-coordination (η^6) by an aryl group, *viz.* [K(MesForm)(MesFormH)] (MesForm = N(Mes)C(H)N(Mes), Mes = 2,4,6-$Me_3C_6H_2$) [7]. In this particular instance the coordination mode exhibited by the amidinate is also exhibited by a neutral E-syn amidine that co-coordinates the metal centre (Scheme 1). Indeed, such is the stability of this complex that the neutral formamidine resists deprotonation using a 10-fold excess of potassium hexamethyldisilazide (K-HMDS, H-HMDS p$K_a \sim 30$) [8] or potassium hydride (H_2 p$K_a \sim 35$) [8]. At this time we proposed that the suppressed reactivity arises from the steric bulk of the *N*-substituents, which disfavour typical *N*,*N*′-chelation [9], the increased π-donor ability of the aryl groups (cf. alkyl substitution), and the larger coordination sphere of potassium (ionic radius 1.36 Å) [10] which complements the increased bite angle of this binding mode vis-a-vis N,N-chelation. An extension of this study to the ultra bulky N(Dipp)C(H)NH(Dipp) ligand (=DippForm) gave an identical *N*:*aryl*-amidinate binding mode,

* Corresponding author. Fax: +61 (0)3 9905 4597.
E-mail address: peter.junk@sci.monash.edu.au (P.C. Junk).

0022-328X/$ - see front matter © 2007 Elsevier B.V. All rights reserved.
doi:10.1016/j.jorganchem.2007.02.028

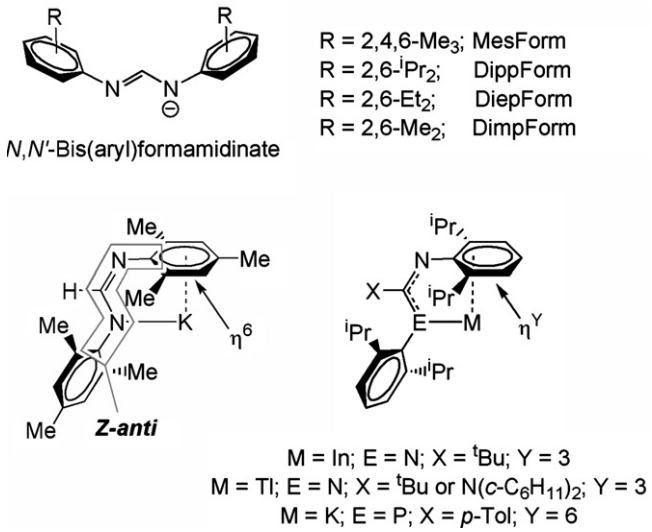

Fig. 1. Overview of bulky *N*,*N*′-bis(aryl)formamidinates referred to in this article and graphic illustration of the *Z-anti* [6] formamidinate binding mode in [K(MesForm)(MesFormH)] (lower left) and known monovalent heavy group 13 pivamidinate (X = ^{t}Bu), guanidinate (X = N(*c*-C_6H_{11})$_2$) and potassium N,P-benzamidinate species bearing an *N*:*aryl*-coordinated amidinate (lower right).

however the decrease in alkyl substituents on the arene, two *vs* three, and increased bulk at the *ortho*-positions, 2,6-disopropyl *vs* 2,4,6-trimethyl, diminishes the impediment to deprotonation resulting in the polymer [{K(THF)$_2$K(DippForm)$_2$}$_n$] (Scheme 1) [11].

During the intervening period since these reports, we have disclosed several other examples of the *Z-anti* [6] *N*:*aryl*-amidinate binding mode with varying metal to π-arene hapticities. These include lithium and sodium species using the formamidinate N(Diep)C(H)N(Diep) (=DiepForm, Diep = 2,6-$Et_2C_6H_3$) [12], the application of pivamidinate [4c] and *N*,*N*-dicyclohexylguanidinate [4d] variants of DippForm to monovalent group 13 chemistry, and preparation of a potassium metallated *N*,*P*-benzamidinate analogue of DippForm (Fig. 1) [13]. We now extend our potassium study of *N*,*N*′-bis(aryl)formamidines to DiepFormH, and report [K(DiepForm)(DiepFormH)] (**1**), which exhibits suppressed reactivity with K-HMDS, and the isolation of complexes pertinent to a study of the limits of suppressed K-HMDS reactivity for bulky *N*,*N*′-bis(aryl)formamidines with K-HMDS.

2. Results and discussion

(i) *DiepFormH and K-HMDS*

The 1:1 stoichiometric treatment of a THF solution of DiepFormH with 0.5 M K-HMDS in toluene (Scheme 1; **1**) results in incomplete deprotonation of the amino group as evidenced by a shifting and broadening of the infrared C=N stretch of the formamidine from 1635 cm^{-1} [14] to 1622 cm^{-1} and retention of a strong N–H stretch at 3156 cm^{-1}. Removal of DiepFormH by washing with toluene, a solvent used for the recrystallisation of DiepFormH, proved unsuccessful suggesting incorporation of the neutral amidine in the product, **1**. Compound **1** was found to be sparingly soluble in C_6D_6, a solvent that freely dissolves DiepFormH.

Unlike the parent amidine, which displays fluxional interconversion between *Z-anti*/*E-syn* and *E-anti* isomeric forms [6] at ambient temperature (C_6D_6) [14], a d_8-THF ^{1}H NMR spectrum of **1** describes a single Diep environment, partial resonance broadening and an N–H resonance (5.97 ppm) that integrates as 0.5H relative to prominent Diep signals (e.g. 24H CH_3 triplet at 1.15 ppm). The addition of 0.5 molar equivalents of K-HMDS to a THF solution of DiepFormH also gives a product that characterises (^{1}H NMR and IR) as **1**.

The partial deprotonation of DiepFormH and *single* Diep environment of **1** are reminiscent of data acquired for [K(MesForm)(MesFormH)] (Scheme 1) [7]. However, compound **1** possesses a single NC(H)N resonance at 7.44 ppm that is considerably upfield of the two distinct resonances (8.22 and 9.13 ppm) observed for the MesForm/MesFormH compound at −80 °C in C_6D_6 (cf. NC(H)N 6.89 ppm for *Z-anti*/*E-syn* [6] DiepFormH in C_6D_6) [14]. Attempts to obtain analogous low temperature data for **1** were thwarted by low solubility, as was the collection of an ambient temperature ^{13}C{^{1}H} NMR spectrum. The collection of ^{13}C{^{1}H} NMR data at high temperature gave broadened, poor quality, spectra.

Further to spectroscopic characterisation, recrystallisation of vacuum dried samples of **1** from fresh toluene gave colourless crystals of two distinct morphologies; one rhombohedral prismatic, the other hexagonal plates. Both morphologies were of suitable quality for single crystal X-ray structure determination and, as illustrated in Figs. 2 and 3, this identified them as [K(DiepForm)(DiepFormH)(THF)]

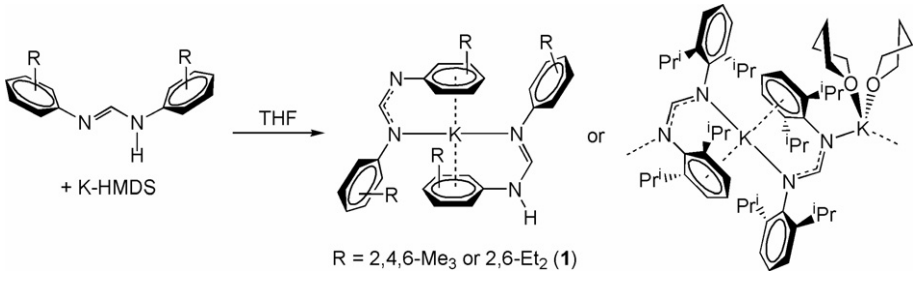

Scheme 1. Preparation of known bulky formamidinate complexes of potassium and compound **1** (by-product of syntheses = H-HMDS).

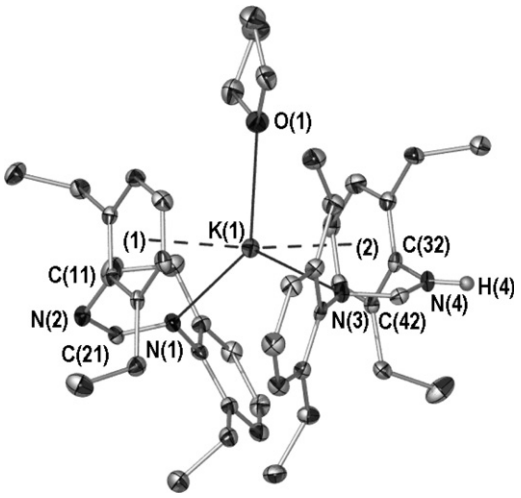

Fig. 2. Molecular structure of **1**(THF) (POV-Ray illustration, 40% thermal ellipsoids). All hydrogen atoms except H(4) omitted for clarity. Selected bond lengths and angles listed in Tables 3 and 4.

(**1**(THF)) and [K(DiepForm)(DiepFormH)] · tol (**1** · tol) respectively. Table 1 contains a summary of crystallographic data for **1**(THF) and **1** · tol. Tables 3 and 4 provide selected bond lengths and angles for all compounds reported herein and related literature species (see reference key).

Variations between the molecular structures of **1**(THF) and **1** · tol principally arise due to the increased coordination number of the former (**1**(THF); K–O_{THF} 2.841(3) Å). This results in extended potassium donor contacts, e.g. K–N and K–aryl centroid (see Table 3). Both complexes comprise a 'metallocene' like K(formamidine/ate)$_2$ unit containing two ligands that chelate the potassium by *N*-donation and η^6-arene coordination. Like [K(MesForm)(MesFormH)] [7], intermolecular H-bonding (see Fig. 3 for **1** · tol example) occurs for both species (Tables 3 and 4). Chelation of potassium by the DiepForm ligand is accompanied by C–N and C=N NC(H)N backbone bond lengths suggestive of delocalisation (**1**(THF); 1.316(5), 1.325(4) Å, **1** · tol; 1.322(4), 1.322(4) Å). This agrees with similar bond distances in the MesForm ligand of [K(MesForm)(MesFormH)] (1.319(2), 1.324(2) Å) [7] and the formamidinate ligands of [{K(THF)$_2$K(DippForm)$_2$}$_n$] (1.321(6), 1.315(6) Å) [11]. The DiepFormH ligands of **1**(THF) and **1** · tol possess NC(H)N backbone lengths approaching C–N and C=N bond localisation (**1**(THF); 1.294(5), 1.344(4) Å, **1** · tol; 1.288(4), 1.340(4) Å, DiepFormH; 1.281(3) and 1.352(3) Å) [14]. The K–N contacts differ with the anionic or neutral nature of the ligands (**1**(THF); 2.866(3) *vs* 2.908(3) Å, **1** · tol; 2.745(3) *vs* 2.839(3) Å respectively) and suggest increased steric buttressing relative to [K(MesForm)(MesFormH)] (2.7187(17) *vs* 2.7458(16) Å) [7]. Furthermore, the metal-to-arene centroid distances of **1**(THF) (2.997(11) and 3.108(11) Å) and **1** · tol (2.879(9) and 2.931(9) Å) reflect poorer overall π-donation to the metal relative to [K(MesForm)(MesFormH)] (2.8867(77) and 2.8954(75) Å) [7]. Both complexes possess atom–atom contacts that are shorter than those of [{K(THF)$_2$K(DippForm)$_2$}$_n$] with the exception of the potassium–arene centroid distance of the DiepFormH in higher coordinate **1**(THF) (3.108(11) *vs* 3.034(9) Å) [11].

The attempted synthesis of [K(DippForm)(DippFormH)] in THF using 0.5 M equiv. of K-HMDS gives [K(DippForm)(THF)$_3$].DippFormH [11], which contains a *Z-anti* [6] *N*:*aryl*-coordinated DippForm ligand (η^6) that acts as a hydrogen bond acceptor to the N–H of an unreacted *E-syn* DippFormH [11]. Thus, for **1**, it appears the reduced steric bulk of Diep permits a potassium–arene interaction for DiepFormH of sufficient strength to resist substitution by THF [11], and thereby suppressed DiepFormH reactivity. By contrast, the bulkiness of Dipp in "[K(DippForm)(DippFormH)]" destabilises the metal–arene interaction, enabling full deptrotonation by K-HMDS [11].

(ii) *Reaction of* **1** *with n-BuLi*

The stability of **1**, and the retention of the *N*:*aryl*-coordinated K(Formamidine/ate)$_2$ unit in [{K(THF)$_2$K(DippForm)$_2$}$_n$] [11], led us to pursue the deprotonation of **1** to

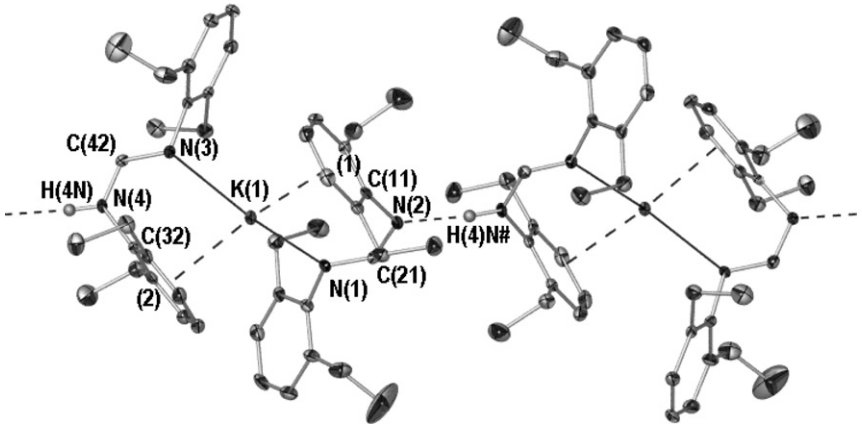

Fig. 3. Molecular structure of **1** · tol illustrating hydrogen bonding to adjacent units (POV-Ray illustration, 40% thermal ellipsoids). All hydrogen atoms except H(4)N omitted for clarity. Symmetry transformation used to generate '#' atoms: $\frac{1}{2}-x$, $\frac{3}{2}-y$, $\frac{1}{2}+z$. Selected bond lengths and angles listed in Tables 3 and 4.

Table 1
Summary of crystal data for compounds **1**(THF), **1** · tol, **2** and **4**

	[K(DiepForm/H)$_2$(THF)] (**1**(THF))	[K(DiepForm/H)$_2$] · tol (**1** · tol)	[{Li(THF)$_2$K(DiepForm)$_2$}$_n$] (**2**)	[{K$_3$(DimpForm)$_3$(DME)$_3$}$_n$] (**4**)
Mol. formula	$C_{46}H_{63}KN_4O$	$C_{49}H_{63}KN_4$	$C_{100}H_{140}K_2Li_2N_8O_4$	$C_{63}H_{87}K_3N_6O_6$
Mol. weight	727.10	747.13	1610.28	1141.69
Temperature (K)	123(2)	123(2)	123(2)	123(2)
Space group	$P2_1/n$	$P2_1/n$	*Pbca*	$P2_1/c$
a (Å)	14.6182(5)	15.8628(5)	19.6451(4)	17.5290(4)
b (Å)	17.7100(6)	17.5444(6)	43.4403(10)	17.9710(4)
c (Å)	16.9473(6)	16.2912(6)	21.9380(4)	20.9367(5)
α (°)	90	90	90	90
β (°)	96.833(2)	96.8220(10)	90	91.300(10)
γ (°)	90	90	90	90
Volume (Å^3)	4356.3(3)	4501.8(3)	18721.7(7)	6593.6(3)
Z	4	4	8	4
D_c, g cm^{-3}	1.109	1.102	1.143	1.150
μ (mm^{-1})	0.159	0.154	0.155	0.257
Reflections collected	27184	46960	59436	64639
Unique reflections	9353	11011	13516	15854
Parameters varied	477	507	1061	740
R_{int}	0.2313	0.2077	0.2732	0.2352
R_1	0.0639	0.0810	0.0775	0.0835
wR_2	0.1230	0.1428	0.0900	0.1774

yield [K(DiepForm)$_2$]$^-$ as a stable anion. To this end, a THF solution of **1** was treated with an equimolar quantity of *n*-BuLi (*n*-butane pK_a ~ 50–55) [8] (Scheme 2). Removal of reaction volatiles gave a colourless highly air- and moisture sensitive powder (**2**) devoid of IR stretches attributable to **1** (IR C=N; **1** 1622 cm^{-1}, **2** 1661 cm^{-1}) and an N–H resonance (**1** d_8-THF ^{1}H NMR; 5.97 ppm). Spectral comparison with [Li$_2$(DiepForm)$_2$(THF)$_3$] (IR C=N; 1607 cm^{-1}) indicates that **2** is a new species, as do the relative thermal stabilities of **1**, **2** and [Li$_2$(DiepForm)$_2$(THF)$_3$] (m.p. **1**; 260 °C, **2**; 329–335 °C, [Li$_2$(DiepForm)$_2$(THF)$_3$]; 134 °C (dec.)) [12]. Recrystallisation of **2** from THF gave colourless rhombohedral prisms of suitable quality for single crystal X-ray structure determination (see Tables 1, 3, 4 and reference key).

As illustrated in Fig. 4, **2** is comprised of *N*:*aryl*-coordinated K(DiepForm)$_2$ 'anions' tethered into a one-dimensional polymer by Li(THF)$_2$ 'cations'. This system bears a structural resemblance to [{K(THF)$_2$K(DippForm)$_2$}$_n$] [12]; salient differences being a reduction in *intra*-anion K–N and K–centroid distances for **2** which correspond to a reduction in aryl bulk (Table 3). Direct comparison with **1** · tol, which possesses the same potassium coordination environment as **2**, reveals an increase in K–N$_{amide}$ bond lengths (**1** · tol; 2.745(3) Å *vs* **2**; 2.805(7) and 2.767 (7) Å) and unexpectedly shorter K(Form)$_2$ unit potassium–arene centroid distances (Table 3). This emphasises the preference of potassium for arene donors despite the free availability of O-(THF) and N-donors (imine) [15]. The NCN formamidinate backbone angles of **2** correlate well with those of [{K(THF)$_2$K(DippForm)$_2$}$_n$] (**2**); 129.1(10)°, 127.8(10)°, [{K(THF)$_2$K(DippForm)$_2$}$_n$]; 128.3(4)° [11] and contrast the related angles of the neutral DiepFormH and MesFormH ligands in **1** · tol and [K(MesForm)(MesFormH)] (**1** · tol; 123.3(3)°, [K(MesForm)(MesFormH)]; 124.78(17)° [7]).

(iii) *Preparation of* **1** *in the presence of DME or PMDETA*

The use of chelating/multidentate amines and ethers to increase the reactivity of bases, e.g. organolithium reagents, is a common practice [16] when using organometallic reagents in synthesis. Conventional wisdom suggests this enhancement results from deaggregation of discrete oligomers, e.g. [{Li(μ$_3$-^{n}Bu)(THF)}$_4$] [17], to lower nuclearity species, e.g. [{Li(μ-^{n}Bu)(η^2-TMEDA)}$_2$] (TMEDA = *N*,

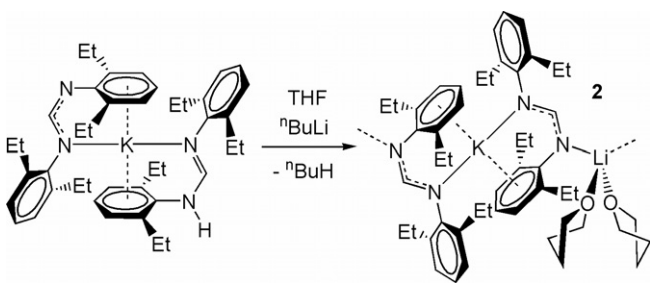

Scheme 2. Preparation of polymeric lithium–potassium formamidinate **2**.

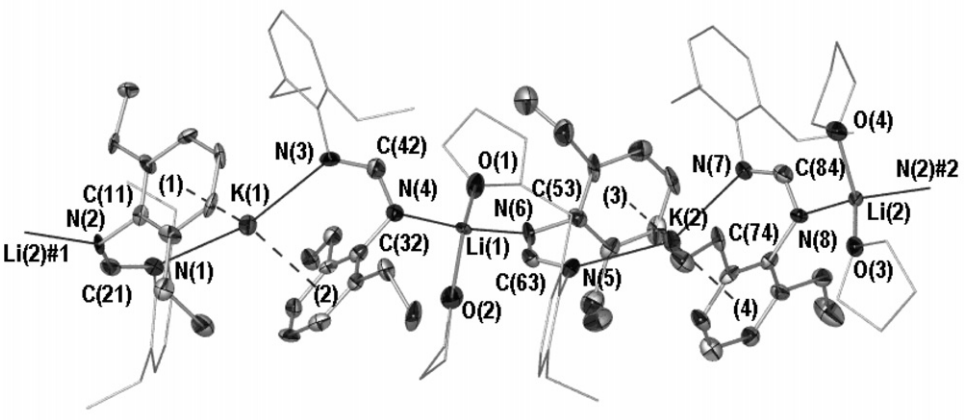

Fig. 4. Molecular structure of **2** (POV-Ray illustration, 40% thermal ellipsoids). All hydrogen atoms omitted for clarity. Non-coordinating aryl and THF hydrocarbyl groups depicted as wire frames. Symmetry transformations used to generate equivalent atoms: #1 $\frac{1}{2}-x,\ y-\frac{1}{2},\ z$; #2 $\frac{1}{2}-x,\ \frac{1}{2}+y,\ z$. Selected bond lengths and angles listed in Tables 3 and 4.

N,*N*′,*N*′-tetramethylethylenediamine) [17,18], that increase the rate of reaction by cooperative or competitive solvation [16,19]. While the influence of solvation on organolithium reagents has been widely studied [20], the influence of chelating solvents on the basicity of amides or heavier alkali metal species has received less attention. Indeed, to our knowledge, the enhancement of K-HMDS reactivity by chelating donors has not been studied. Our original communication of the attenuated reactivity of MesFormH toward K-HMDS and KH included a failed attempt to enhance the reactivity of these bases using TMEDA [7]. Similarly, the addition of TMEDA (10.0 equiv.) to preparation media for **1** failed to generate a "K(DiepForm)" species nor a TMEDA-solvated **1**, as evidenced by infrared and ^{1}H NMR spectroscopies. With this in mind, our attention turned to the introduction of the less sterically encumbered bidentate ether 1,2-dimethoxyethane (DME) and the triamine *N*,*N*,*N*′,*N*″,*N*″-pentamethyldiethylenetriamine (PMDETA) to THF preparation media for **1** (*ca.* 12 and 7 equiv. respectively). We targeted DME due to its relative size to THF, the congestion of **1**(THF) and the widespread use of DME as a chelate donor in potassium chemistry. The amine PMDETA was chosen because of its tridentate nature.

As illustrated in Schemes 3 and 4 respectively, reaction of DiepFormH with an equimolar quantity of K-HMDS in the presence of DME or PMDETA results in complete deprotonation of the formamidine to give

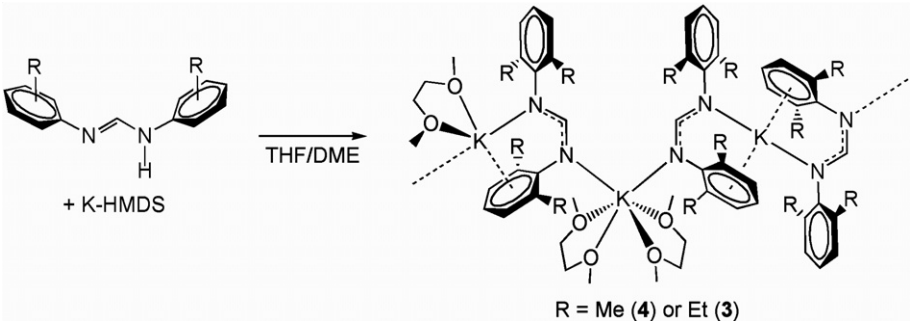

Scheme 3. Preparation of DME compounds **3** and **4** (by-product of syntheses = H-HMDS).

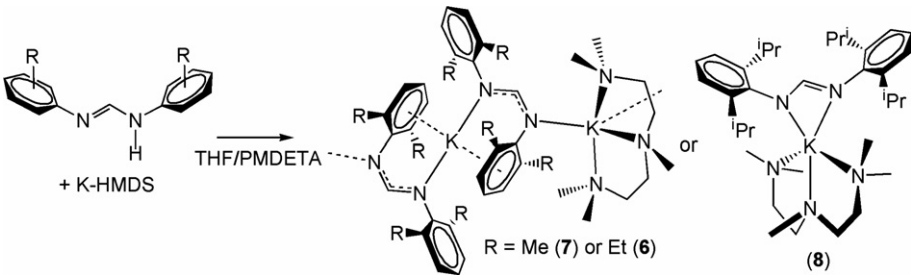

Scheme 4. Preparation of PMDETA compounds **6**–**8** (by-product of syntheses = H-HMDS).

$[\{K_3(DiepForm)_3(DME)_3\}_n\}] \cdot \frac{n}{4}DME$ (**3**) and $[\{K(PMDETA)K(DiepForm)_2\}_n] \cdot n$-toluene (**6** · tol) vide infra. ^1H NMR spectra of both species (C_6D_6) indicate single DiepForm 'Diep' environments, as per **1**, with a well defined NC(H)N singlet at 7.43 and 7.87 ppm respectively (cf. **1** d_8-THF; 7.44 ppm). Direct comparison with related data for the less sterically hindered compounds $[\{K_2(\mu{:}\eta^2{:}\eta^2\text{-}p\text{TolForm})(\mu{:}\eta^2{:}\eta^1\text{-DME})_2\}_n]$ (pTolForm = N(pTol)C(H)N(pTol), pTol = *para*-tolyl) and [K(pTolForm)(18-crown-6)] (NC(H)N; 8.61 and 9.15 ppm respectively) [9], which incorporate *E-anti* formamidinates, as-well-as that of **1** (*Z-anti*) [6] leads to the supposition that an NC(H)N ^1H NMR signal at *ca.* 7.50 ppm in C_6D_6 is consistent with a *Z-anti* formamidinate. Crystalline samples of **3** and **6** · tol suitable for single crystal X-ray diffraction data collection were acquired by concentration of the reaction mother liquor to the point of crystallisation (**3**) or addition of hexane to a concentrated solution (**6** · tol). The data collected for **3** were poor and prohibited full anisotropic refinement. However the connectivity of the compound and its composition were deduced [21]. Similarly, the low quality of data for **6** · tol, disorder of 2,6-ethyl substituents and disorder of lattice toluene led to a poor quality refinement (Table 2). Repeat syntheses of **3** and **6** using the comparable formamidine (Dimp)N=(H)NH(Dimp) (=DimpFormH, Dimp = 2,6-$Me_2C_6H_3$, Schemes 3 and 4) gave the lattice solvent free DimpForm analogues; $[\{K_3(DimpForm)_3(DME)_3\}_n]$ (**4**) and $[\{K(PMDETA)K(DimpForm)_2\}_n]$ (**7**), for which good quality X-ray data were acquired (Tables 1 and 2). Spectroscopic data for **4** and **7** were consistent with **3** and **6** · tol with the absence of non-coordinating solvent (see Section 4).

Table 2
Summary of crystal data for compounds **6** · tol, **7** and **8**

	$[\{K(PMDETA)K(DiepForm)_2\}_n] \cdot n$tol (**6** · tol)	$[\{K(PMDETA)K(DimpForm)_2\}_n]$ (**7**)	[K(DippForm)(PMDETA)] (**8**)
Mol. formula	$C_{58}H_{85}K_2N_7$	$C_{43}H_{61}K_2N_7$	$C_{34}H_{58}KN_5$
Mol. weight	958.53	754.19	575.95
Temperature (K)	123(2)	123(2)	123(2)
Space group	$P2_1/c$	$P2_12_12_1$	*Pnma*
a (Å)	19.9794(4)	12.9687(3)	21.0653(17)
b (Å)	14.8132(3)	17.0431(4)	19.7737(12)
c (Å)	21.6504(5)	20.3504(6)	17.1371(12)
α (°)	90	90	90
β (°)	116.0430(10)	90	90
γ (°)	90	90	90
Volume (Å^3)	5757.0(2)	4498.0(2)	7138.3(9)
Z	4	4	8
D_c (g cm^{-3})	1.106	1.114	1.072
μ (mm^{-1})	0.205	0.246	0.177
Reflections collected	50758	27719	39062
Unique reflections	15877	10673	7348
parameters varied	661	482	406
R_{int}	0.1159	0.0983	0.1558
R_1	0.0839	0.0599	0.0918
wR_2	0.2073	0.1010	0.2019

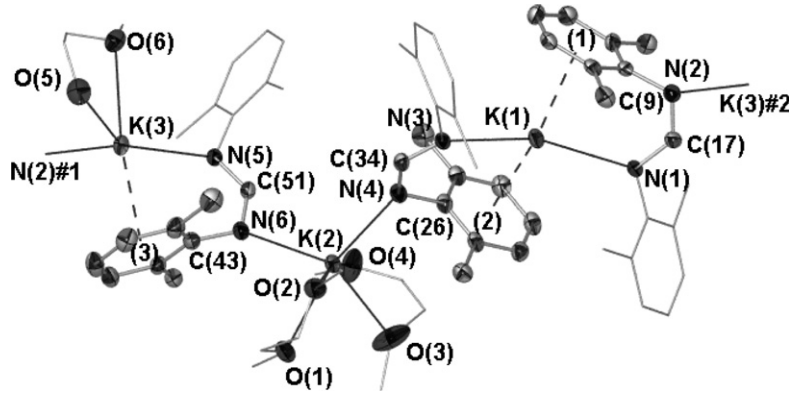

Fig. 5. Molecular structure of **4** (POV-Ray illustration, 40% thermal ellipsoids). All hydrogen atoms omitted for clarity. Non-coordinating aryl and DME hydrocarbyl groups depicted as wire frames. Symmetry transformations used to generate equivalent atoms: #1 $1+x, y, z$; #2 $x-1, y, z$. Selected bond lengths and angles listed in Tables 3 and 4.

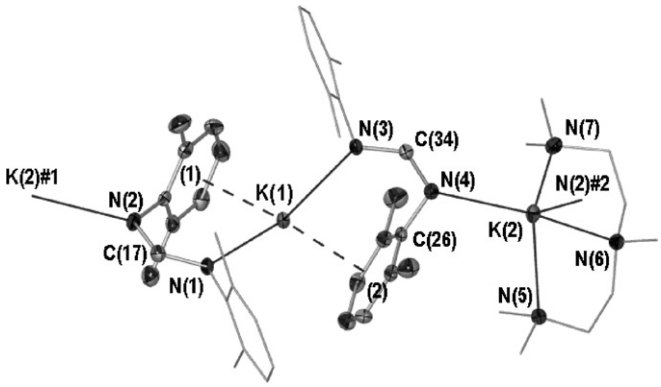

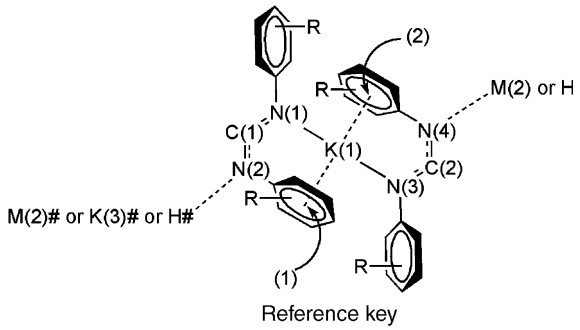

Fig. 6. Molecular structure of **7** (POV-Ray illustration, 40% thermal ellipsoids). All hydrogen atoms omitted for clarity. Non-coordinating aryl and PMDETA hydrocarbyl groups depicted as wire frames. Symmetry transformations used to generate equivalent atoms: #1 $x-1/2,\ -y,\ z-1/2$; #2 $-x-1/2,\ -y,\ 1/2-z$. Selected bond lengths and angles listed in Tables 3 and 4.

As illustrated in Figs. 5 and 6, compounds **4** and **7** include *Z-anti* [16] formamidinates. Both contain '$K(Form)_2$' units tethered into one-dimensional polymers reminiscent of compound **2** and $[\{K(THF)_2K(DippForm)_2\}_n]$ [11] using the non-$K(Form)_2$ bound nitrogens to coordinate bridging $K(solvent)_n$ units. For **7**, this provides a structure that differs simply in the tethering unit, i.e. K(PMDETA) vis-à-vis $M(THF)_2$ (M = Li or K) [11].

The structure of **4** (and **3** *vide supra*) incorporates a further K(Form)(DME) bridging unit beyond the *pseudo* $K(Form)_2$ 'anion' and $K(solvent)_n$ 'cation' of **2** and **7** (and **6** *vide supra*) to generate an ABC block copolymer. These repeat in the order $K(Form)_2$(=A), $K(DME)_2$ (=B) then K(Form)(DME) (=C), with the 'new' unit bearing a close structural resemblance to the η^6-aryl *Z-anti* [16] formamidinate species $[\{Na(DiepForm)(THF)\}_n]$ and η^1-aryl *Z-anti* component of $[Li(THF)_3Li(DiepForm)_2]$ [12]. Noteworthy differences between **2**, **4** and **7** are the shortening of the intra-$K(Form)_2$ K–N and K–centroid distances in the all-potassium compounds indicating, as expected, that the $K(Form)_2$ units of compound **2** carry a greater anionic charge (Table 3). Furthermore, the centroid–K–cen-

Table 3
Selected distances (Å) for known bulky formamidinate complexes of potassium and compounds reported herein (see reference key)

	1(THF)[a]	**1** · tol[a]	$[K(H/MesForm)_2]$ [7]	$[K(THF)_2K(DippForm)_2]$ [11]	**2**[b]	**4**[c]	**6** · tol[d]	**7**[e]
K(1)–N(1)	2.866(3)	2.745(3)	2.7187(17)	2.863(4)	2.805(7)	2.766(3)	2.767(3)	2.746(3)
K(1)–N(3)	2.908(3)	2.839(3)	2.7458(16)	2.863(4)	2.767(7)	2.775(3)	2.780(3)	2.770(3)
K(1)–(1)[f]	2.997(11)	2.897(9)	2.8867(77)	3.034(9)	2.885(19)	2.946(9)	2.894(7)	2.921(10)
K(1)–(2)[f]	3.108(11)	2.931(9)	2.8954(75)	3.034(9)	2.870(19)	2.896(9)	2.873(8)	2.897(10)
K(1)–O(1)	2.841(3)	–	–	–	–	–	–	–
M(2)–N(2)#/N(6)	–	–	–	2.687(4)	2.005(14)	2.743(3)	2.754(3)	2.731(3)
M(2)–N(4)	–	–	–	2.687(4)	2.050(15)	2.758(3)	2.734(3)	2.725(3)
N(2)#···H	1.91	1.95	1.80	–	–	–	–	–
N(2)#···N(4)	2.786(4)	2.827(3)	2.663(2)	–	–	–	–	–
M(2)–D(1)[g]	–	–	–	2.668(5)	1.993(13)	2.745(3)	2.788(4)	2.851(3)
M(2)–D(2)[g]	–	–	–	2.667(6)	2.067(13)	2.814(3)	2.904(4)	2.928(3)
M(2)–D(3)[g]	–	–	–	–	–	2.789(4)	2.843(4)	2.929(3)
M(2)–D(4)[g]	–	–	–	–	–	2.867(3)	–	–
K(3)–(3)[f]	–	–	–	–	–	3.068(9)	–	–
K(3)–N(5)	–	–	–	–	–	2.734(3)	–	–
K(3)–N(2)#	–	–	–	–	–	2.715(3)	–	–
K(3)–D(5)[g]	–	–	–	–	–	2.756(3)	–	–
K(3)–D(6)[g]	–	–	–	–	–	2.819(3)	–	–
C(1)–N(1)[h]	1.316(5)	1.322(4)	1.319(2)	1.321(6)	1.311(9)	1.331(5)	1.312(4)	1.317(5)
C(1)–N(2)[h]	1.325(4)	1.322(4)	1.324(2)	1.315(6)	1.314(9)	1.303(5)	1.302(5)	1.319(5)
C(2)–N(3)[h]	1.294(5)	1.288(4)	1.292(2)	1.321(6)	1.309(9)	1.330(5)	1.313(4)	1.321(4)
C(2)–N(4)[h]	1.344(4)	1.340(4)	1.334(2)	1.315(6)	1.313(9)	1.313(5)	1.308(5)	1.299(4)
C(3)–N(5)[h]	–	–	–	–	–	1.324(5)	–	–
C(3)–N(6)[h]	–	–	–	–	–	1.312(5)	–	–

Symmetry transformations used to generate N(2)# atoms: [a] $x-\frac{1}{2},\ \frac{3}{2}-y,\ z-\frac{1}{2}$; [c] $x+1,\ y,\ z$; [d] $x,\ \frac{1}{2}-y,\ z-\frac{1}{2}$; [e] $-x-\frac{1}{2},\ -y,\ z+\frac{1}{2}$.

[b] Parameters listed solely those of lowest numbered molecular unit. M(2) = Li(1). No symmetry transformations used.

[f] (1), (2) and (3) represent centroids of aryl donors, number sequence matches numerical order of ligands in displayed figure.

[g] 'D' refers to DME or PMDETA donor atom, number sequence matches numerical order of relevant figure.

[h] C(1), C(2), C(3) refer to formamidinate methine carbons, number sequence matches numerical order of relevant figure.

Table 4
Selected angles (°) for known bulky formamidinate complexes of potassium and compounds reported herein (see reference key)

	1(THF)[a]	**1** · tol[a]	[K(H/MesForm)$_2$] [7]	[K(THF)$_2$K(DippForm)$_2$] [11]	**2**[b]	**4**[c]	**6** · tol[d]	**7**[e]
N(1)–K(1)–N(3)	123.63(9)	138.39(8)	112.34(5)	180.0	151.3(2)	146.53(10)	147.54(9)	131.73(9)
(1)–K(1)–(2)[f]	173.6(3)	154.1(3)	122.62(23)	180.0	154.4(8)	158.4(3)	148.0(3)	138.6(3)
Ar:Ar interplane	5.4(1)	24.4(1)	48.2(1)	0.0	27.2(4)	15.7(2)	30.0(2)	35.0(1)
N(4)–M(2)–N(2)#/N(6)	–	–	–	149.5(2)	121.2(8)	117.49(10)	114.75(10)	107.43(10)
N(4)–H–N(2)#	171.62	174.20	166.2	–	–	–	–	–
N(2)#–K(3)–N(5)	–	–	–	–	–	114.43(10)	–	–
N(2)#–K(3)–(3)[f]	–	–	–	–	–	104.8(2)	–	–
(3)–K(3)–D(5)[f,g]	–	–	–	–	–	110.3(2)	–	–
(3)–K(3)–D(6)[f,g]	–	–	–	–	–	163.5(2)	–	–
D(1)–M(2)–D(2)[g]	–	–	–	113.1(2)	97.7(7)	61.19(9)	64.34(14)	61.44(8)
D(1)–M(2)–D(3)[g]	–	–	–	–	–	74.28(13)	113.35(13)	108.49(8)
D(1)–M(2)–D(4)[g]	–	–	–	–	–	143.89(10)	–	–
D(2)–M(2)–D(3)[g]	–	–	–	–	–	108.67(11)	62.06(15)	62.49(8)
D(2)–M(2)–D(4)[g]	–	–	–	–	–	163.30(11)	–	–
D(3)–M(2)–D(4)[g]	–	–	–	–	–	58.68(11)	–	–
D(5)–K(3)–D(6)[g]	–	–	–	–	–	59.45(10)	–	–
N(1)–C(1)–N(2)[h]	127.3(4)	126.5(3)	126.30(18)	128.3(4)	129.1(10)	128.2(4)	128.1(3)	126.8(3)
N(3)–C(2)–N(4)[h]	124.4(4)	123.3(3)	124.78(17)	128.3(4)	127.8(10)	127.0(4)	128.3(3)	128.6(4)
N(5)–C(3)–N(6)[h]	–	–	–	–	–	128.0(4)	–	–

Symmetry transformations used to generate N(2)# atoms: [a] $x-\frac{1}{2},\ \frac{3}{2}-y,\ z-\frac{1}{2}$; [c] $x+1,\ y,\ z$; [d] $x,\ \frac{1}{2}-y,\ z-\frac{1}{2}$; [e] $-x-\frac{1}{2},\ -y,\ z+\frac{1}{2}$.
[b] Parameters listed solely those of lowest numbered molecular unit. M(2) = Li(1). No symmetry transformations used.
[f] (1), (2) and (3) represent centroids of aryl donors, number sequence matches numerical order of ligands in displayed figure.
[g] 'D' refers to DME or PMDETA donor atom, number sequence matches numerical order of relevant figure.
[h] C(1), C(2), C(3) refer to formamidinate methine carbons, number sequence matches numerical order of relevant figure.

troid angle of **7** is *ca.* 20° less than those of **2** and **4** (138.6(3)° *vs* 154.4(8)° and 158.4(3)° respectively) (Table 4). This is consistent with increased steric buttressing with the tridentate 'cation' support ligand and coincides with a decreased N_{imine}–M(2)–N_{imine} angle for **7** (Tables 3 and 4). The two *Z-anti* [6] DimpForm containing units of **4** display K–centroid distances that are longer for the 'K(Form)$_2$' unit (Table 3). This reflects the increased coordination number of the 'neutral' K(Form)DME unit relative to the K(Form)$_2$ unit (Table 3).

(iv) *Extension of (iii) to DippForm*

The syntheses of compounds **3** and **6** were repeated using the formamidine DippFormH in order to provide a direct comparison between THF [11], DME and PMDETA solvated complexes. To this end, the complexes [{K(DippForm)(DME)}$_n$] ('*n*' unknown) (**5**) and [K(DippForm)(PMDETA)] (**8**) were prepared using identical procedures to those in (iii) (see Scheme 4 for **8**) and purified by recrystallisation from a concentrated solution (**5**) or placement at −15 °C (**8**). The ^{1}H NMR spectra of both indicate *Z-anti* [6] DippForm ligands on the basis of NC(H)N resonance location (7.76 (C_6D_6) and 7.35 (d_8-THF) ppm respectively) [11].

Unlike compound **5**, for which twinning of crystalline samples repeatedly frustrated X-ray structure determination, crystalline samples of compound **8** were of sufficient quality for full data collection (Fig. 7, selected bond lengths and angles given in Figure caption). Contrary to compounds **1**–**4**, PMDETA solvated complexes **6** and **7** and formamidinate binding mode predictions based on solution ^{1}H NMR spectra (see above), compound **8** crystallises as

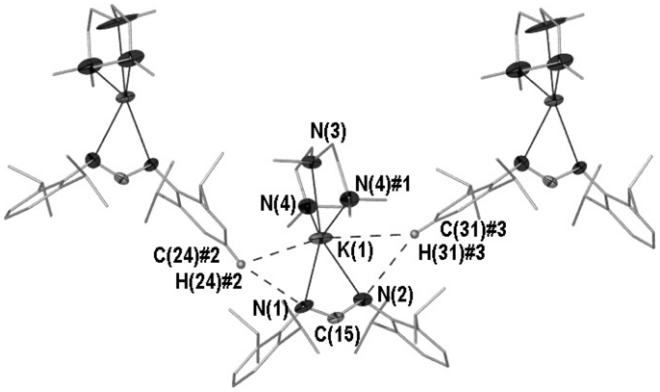

Fig. 7. Molecular structure of **8** illustrating potential interactions with adjacent units (POV-Ray illustration, 40% thermal ellipsoids). All hydrogen atoms except H(24)#2 and H(31)#3 omitted for clarity. All hydrocarbyl groups except NCN methine depicted as wire frames. Symmetry transformations used to generate equivalent atoms: #1 $x,\ \frac{1}{2}-y,\ z$; #2 $\frac{1}{2}-x,\ \frac{1}{2}-y,\ \frac{1}{2}-z$; #3 $x+\frac{1}{2},\ \frac{1}{2}-y,\ \frac{3}{2}-z$. Selected distances (Å) and angles (°): K(1)–N(1) 2.692(6), K(1)–N(2) 2.844(6), K(1)–N(3) 2.899(6), K(1)–N(4) 2.811(5), K(1)–N(4)#1 2.811(5), N(1)–C(15) 1.333(8), N(2)–C(15) 1.295(8), K(1)···H(24)#2 3.36, K(1)···C(24)#2 3.806(11), K(1)···H(31)#3 3.76, K(1)···C(31)#3 4.615(8), K(1)···C(31)#3 4.615(8), N(1)···H(24)#2 2.96, N(1)···C(24)#2 3.869(11), N(2)···H(31)#3 3.26, N(2)···C(31)#3 4.172(10), N(1)–K(1)–N(2) 50.56(19), N(3)–K(1)–N(4) 62.53(11), N(4)–K(1)–N(4)#1 121.0(2), N(1)–K(1)–N(3) 158.2(2), N(2)–K(1)–N(3) 151.2(2), N(1)–C(15)–N(2) 128.6(7), K(1)···H(24)#2–C(24)#2 111.3, N(1)···H(24)#2–C(24)#2 161.3, K(1)···H(31)#3–C(31)#3 151.5, N(2)–H(31)#3–C(31)#3 161.3.

two unique discrete five-coordinate monomers (only first discussed herein) with extended potassium to PMDETA central nitrogen contacts (2.899(6) Å) and disparate potassium to *E-anti* [6] chelating formamidinate nitrogen

distances (2.692(6) and 2.844(6) Å). The *ca.* 0.15 Å disparity suggests asymmetry in the NCN backbone of the DippForm ligand. Further to these intramolecular contacts, bifurcated intermolecular interactions between the *para*-CH of each Dipp ring and the potassium and NCN nitrogen of adjacent [K(DippForm)(PMDETA)] units appear to complement the unusual planar donor set of the PMDETA ligand in **8** (Fig. 7). However, these contacts are beyond the combined van der Waals radii (*ca.* 3.00 Å) [10] and the bonding exhibited by the PMDETA of **8** therefore appears to be an artefact of crystal packing.

3. Conclusion

The ligand DiepForm generates *N*:η^6-*aryl*-coordinated potassium compounds containing the 'K(Form/H)$_2$' motif. Combined with *Z-anti* [6] formamidinate coordination of potassium, the hexamethyldisilazide (HMDS) anion cannot effect complete deprotonation of DiepFormH in THF/toluene solution (**1**). Compound **1** can be deprotonated by *n*-BuLi or addition of DME or PMDETA to the preparation medium of **1**. This results in the isolation of AB (**2** and **6**) or ABC (**3**) block copolymers. Extension of this work to DimpForm (**4** and **7**) and DippForm (**5** and **8**) indicates that both behave similarly to DiepForm analogues in solution (cf. ^{1}H NMR NC(H)N resonance at *ca.* 7.50 ppm), but the DippForm complex **8** exists as discrete *N*,*N*′-chelated monomers in the solid-state.

4. Experimental

The *N*,*N*′-bis(aryl)formamidinate ligand precursors *N*,*N*′-bis(2,6-dimethylphenyl)-, *N*,*N*′-bis(2,6-diethylphenyl) and *N*,*N*′-bis(2,6-diisopropylphenyl)formamidine (DimpFormH, DiepFormH and DippFormH respectively) were synthesised according to a modified published procedure [22]. *n*-BuLi (1.6 M in hexane) and potassium hexamethyldisilazide (0.5 M in toluene) were purchased from Aldrich. Tetrahydrofuran (THF) and 1,2-dimethoxyethane (DME) were dried over sodium, freshly distilled from sodium benzophenone ketyl (THF) or sodium (DME) and freeze–thaw degassed prior to use. *N,N,N′,N″,N″*-Pentamethyldiethylenetriamine (PMDETA) was freshly distilled, dried over 3–5 Å molecular sieves and freeze–thaw degassed prior to use. All manipulations were performed using conventional Schlenk or glovebox techniques under an atmosphere of high purity dinitrogen in flame-dried glassware. Infrared spectra were recorded as Nujol mulls using sodium chloride plates on a Perkin Elmer 1600 FTIR spectrophotometer. ^{1}H NMR spectra were recorded at 300.13 MHz and ^{13}C{^{1}H} NMR spectra were recorded at 75.46 MHz using a Bruker AC 300 spectrometer. Chemical shifts were referenced to the residual ^{1}H and ^{13}C resonances of *deutero* benzene (δ_H 7.16 and δ_C 128.39) or methylene resonances of d_8-THF (δ_H 1.73 and 3.58 and δ_C 25.37 and 67.57). Melting points were determined in sealed glass capillaries under dinitrogen. Reproducible microanalyses for compounds **1**–**8** could not be obtained due to inconsistent solvent loss and high air- and moisture sensitivity.

4.1. [K(DiepForm)(DiepFormH)(THF)] (1(THF)) and [K(DiepForm)(DiepFormH)] · toluene (1 · tol)

4.1.1. Method 1

K-HMDS (6.60 mL, 3.30 mmol) was added dropwise to a stirred solution of DiepFormH (1.02 g, 3.31 mmol) in THF (20 mL) to give a rich yellow solution that was left to stir for 16 h. Filtration, concentration to the point of crystallisation (*ca.* 15 mL) and placement at −5 °C gave the title compounds as colourless rhombohedral prisms and hexagonal plates respectively (0.92 g, 74%, 1.23 mmol based on [K(DiepForm)(DiepFormH)] · toluene), m.p. 267 °C. IR: 1900 w, 1839 w, 1763 w, 1622 s, 1533 s, 1256 m, 1190 sh m, 1151 m, 1076 m, 1031 m, 960 w, 918 m, 870 w, 786 m, 758 sh s, 728 sh s, 694 m, 662 w cm^{-1}; ^{1}H NMR (d_8-THF, 300 K, vacuum dried sample): δ 1.15 (t, 24H; CH_3, $^3J_{HH} = 7.3$ Hz), 2.65 (q, 16H; CH_2, $^3J_{HH} = 7.3$ Hz), 5.97 (br s, 1H; NH), 6.62–7.26 (m, 12H; ArH), 7.44 (s, 2H; NC(H)N); Compound too insoluble for satisfactory acquisition of ^{13}C{^{1}H} NMR data.

4.1.2. Method 2

Following the procedure for *Method 1*, K-HMDS (4.00 mL, 2.00 mmol) and DiepForm (1.24 g, 4.02 mmol) gave colourless rhombohedral prisms and hexagonal plates of **1** (0.98 g, 66%, 1.31 mmol based on [K(DiepForm)(DiepFormH)] · toluene), m.p. 260 °C. IR and ^{1}H NMR data consistent with **1** from *Method 1*.

4.2. [{Li(THF)$_2$K(DiepForm)$_2$}$_n$] (2)

n-BuLi (1.20 mL, 1.92 mmol) was added dropwise to a stirred pale yellow solution of in situ prepared **1** (Method 2; 1.18 g, 3.83 mmol DiepFormH, 3.80 mL, 1.90 mmol K{N(SiMe$_3$)$_2$}) in THF (20 mL). The resulting light yellow clear solution was left to stir for 12 h prior to concentration in vacuo (*ca.* 5 mL). Prolonged standing at −15 °C gave **2** as colourless rhombohedral prisms (1.11 g, 1.38 mmol, 73%), m.p. 329–335 °C (decomposition, solvent loss 190 °C). IR: 1920 w, 1861 w, 1801 w, 1745 w, 1661 m, 1593 s, 1534 s, 1228 m, 1189 s, 1103 sh m, 1072 m, 987 m, 961 sh m, 916 s, 866 m, 812 m, 788 s, 757 m, 729 sh m, 694 sh w, 671 m cm^{-1}; ^{1}H NMR (d_8-THF, 300 K): δ 1.16 (t, 24H; CH_3, $^3J_{HH} = 6.6$ Hz), 2.65 (q, 16H; CH_2, $^3J_{HH} = 6.6$ Hz), 6.62–7.12 (m, 12H; ArH), 7.39 (s, 2H; NC(H)N); ^{13}C{^{1}H} NMR (d_8-THF, 300 K): δ 11.6 (s; CH_3), 22.5 (s; CH_2), 119.0 (br s; ArC), 122.8 (s; ArCH), 134.6 (br s; ArCH), 144.9 (br s; ArC), 153.2 (br s; NCN).

4.3. General procedure for [K(Form)(DME)$_x$] compounds 3–5

K-HMDS (6.00 mL, 3.00 mmol) was added dropwise to a stirred solution of *N*,*N*′-bis(aryl)formamidine (3.00 mmol)

in THF/DME (4:1, 20 mL, 38.48 mmol DME). The resulting solution, which ranged from colourless to light yellow in appearance, was stirred for 12 h. Filtration and concentration to the point of crystallisation gave colourless cubes (**3**), irregular prisms (**4**) or a microcrystalline powder (**5**) upon standing. Relevant details for each compound are listed below.

4.3.1. $[\{K_3(DiepForm)_3(DME)_3\}_n\}] \cdot \frac{n}{4} DME$ (**3**)

Isolated yield 0.87 g (65%, 0.65 mmol), m.p. 76 °C. IR: 1929 w 1868 w, 1667 w, 1628 m, 1590 sh m, 1538 s, 1253 m, 1234 m, 1189 sh s, 1102 sh m, 1030 w, 909 sh m, 867 w, 812 m, 788 m, 759 sh m, 725 w cm^{-1}; ^1H NMR (C_6D_6, 300 K): δ 1.15 (t, 36H; CH_3, DiepForm, $^3J_{HH} = 6.2$ Hz), 2.64 (q, 24H; CH_2, DiepForm, $^3J_{HH} = 6.2$ Hz), 3.01 (s, 19$\frac{1}{2}$H; CH_3, DME), 3.19 (s, 13 H; OCH_2, DME), 6.78–7.14 (br m, 18H; ArH), 7.43 (s, 3H; NC(H)N). Compound too insoluble for satisfactory acquisition of $^{13}C\{^1H\}$ NMR data.

4.3.2. $[\{K_3(DimpForm)_3(DME)_3\}_n]$ (**4**)

Isolated yield 0.93 g (81%, 0.81 mmol), m.p. 95 °C (decomposition 129 °C). IR: 1897 w, 1832 w, 1774 w, 1651 m, 1594 m, 1532 s, 1248 s, 1193 s, 1112 s, 1028 s, 984 s, 947 s, 920 sh m, 899 m, 847 s, 812 m, 792 sh m, 756 s, 662 sh m, 621 sh w cm^{-1}; ^1H NMR (C_6D_6, 300 K): δ 2.19 (br s, 36H; CH_3, DimpForm), 3.03 (s, 18 H; CH_3, DME), 3.21 (s, 12H; OCH_2, DME), 6.81–7.07 (br m, 18H; ArH), 7.42 (br s, 3H; NC(H)N). Compound too insoluble for satisfactory acquisition of $^{13}C\{^1H\}$ NMR data.

4.3.3. K(DippForm)(DME) (**5**)

Isolated yield 0.78 g (53%, 1.58 mmol), m.p. 47–52 °C. IR: 1892 w, 1839 w, 1733 w, 1671 sh w, 1594 sh m, 1538 s, 1242 m, 1193 m, 1113 m, 1030 m, 934 sh m, 913 sh m, 856 sh m, 820 w, 798 m, 753 sh m, 721 w cm^{-1}; ^1H NMR (C_6D_6, 300 K): δ 1.32 (d, 24H; CH_3, ^{i}Pr, $^3J_{HH} = 6.9$ Hz), 3.11 (s, 6H; CH_3, DME), 3.30 (s, 8H; CH_2, DME), 3.70 (h, 4H; CH, ^{i}Pr, $^3J_{HH} = 6.9$ Hz), 7.03–7.24 (m, 6H; ArH), 7.76 (br s, 1H; NC(H)N); $^{13}C\{^1H\}$ NMR (C_6D_6, 300 K): δ 24.8 (s; CH_3, ^{i}Pr), 28.5 (s; CH, ^{i}Pr), 58.9 (s; CH_3, DME), 72.5 (s; CH_2, DME), 122.2, 123.4 (s; ArCH), 142.8, 147.1 (s; ArC), 161.5 (s; NCN).

4.4. General procedure for [K(Form)(PMDETA)$_x$] compounds **6**–**8**

K-HMDS (4.00 mL, 2.00 mmol) was added dropwise to a stirred solution of *N*,*N*′-bis(aryl)formamidine (2.00 mmol) in THF/PMDETA (6:1, 20 mL, 13.68 mmol PMDETA). The resulting yellow solution was stirred for 12 h. Filtration, concentration (*ca.* 5 mL) and addition of hexane (**6**, 2 mL) or placement at −15 °C (**7** and **8**) gave colourless triangular prisms (**6**), blocks (**7**) or irregular prisms (**8**) upon standing. Relevant details for each compound are listed below.

4.4.1. $[\{K(PMDETA)K(DiepForm)_2\}_n] \cdot n$ toluene (**6** · tol)

Isolated yield 0.62 g (65%, 0.65 mmol), m.p. 102 °C. IR: 1893 w, 1860 w, 1836 w, 1650 w, 1592 sh m, 1532 s, 1256 m, 1228 m, 1189 s, 1163 w, 1118 w, 1103 m, 1081 m, 1032 m, 931 w, 911 m, 811 sh m, 787 sh m, 756 sh m, 731 sh m, 695 sh w, 673 w cm^{-1}; ^1H NMR (C_6D_6, 300 K): δ 1.40 (t, 24H; CH_3, $^3J_{HH} = 7.5$ Hz), 2.00 (s, 3H; NCH_3), 2.05 (s; 12H; $N(CH_3)_2$), 2.12–2.28 (m, 8H; CH_2CH_2), 2.92 (q, 16H; CH_2, $^3J_{HH} = 7.5$ Hz), 7.01–7.23 (m, 12H; ArH), 7.87 (br s, 2H; NC(H)N); $^{13}C\{^1H\}$ NMR (C_6D_6, 300 K): δ 14.4 (s; CH_3), 24.6 (s; CH_2), 41.0 (s; NCH_3), 44.3 (s; $N(CH_3)_2$), 55.0 (s; CH_2), 56.5 (s; CH_2), 124.4 (s; ArC), 125.1 (s; ArCH), 127.3 (s; ArCH), 128.0 (s; ArC), 153.9 (s; NCN).

4.4.2. $[\{K(PMDETA)K(DimpForm)_2\}_n]$ (7)

Isolated yield 0.66 g (88%, 0.88 mmol), m.p. 148 °C. IR: 1911 w, 1889 w, 1861 w, 1822 w, 1789 w, 1650 w, 1589 sh s, 1533 br s, 1239 m, 1194 s, 1167 m, 1122 m, 1089 s, 1028 s, 978 m, 928 m, 900 m, 800 m, 761 sh s, 722 w, 661 sh w cm^{-1}; ^1H NMR (C_6D_6, 300 K): δ 1.80 (s, 3H; NCH_3), 1.88 (s, 24H; CH_3), 2.00 (m, 8H; CH_2CH_2), 2.27 (br s, 12H; $N(CH_3)_2$), 6.51–6.98 (m, 12H; ArH), 7.18 (br s, 2H; NC(H)N); $^{13}C\{^1H\}$ NMR (C_6D_6, 300 K): δ 19.1 (s; CH_3), 40.2 (s; NCH_3), 44.0 (s; $N(CH_3)_2$), 54.9 (s; CH_2), 56.2 (s; CH_2), 118.9 (s; ArCH), 124.1 (s; ArC), 130.2 (s; ArCH), 136.7 (s; ArC), 155.0 (s; NCN).

4.4.3. [K(DippForm)(PMDETA)] (**8**)

Isolated yield 1.07 g (93%, 1.86 mmol), m.p. 115 °C. IR: 1915 w, 1787 w, 1664 sh m, 1592 sh m, 1535 s, 1257 m, 1234 m, 1178 m, 1129 m, 1099 m, 1080 m, 1034 s, 933 sh m, 915 sh m, 804 sh w, 772 sh m, 761 sh m, 728 w, 694 w cm^{-1}; ^1H NMR (d_8-THF, 300 K): δ 1.16 (d, 24H; CH_3, ^{i}Pr, $^3J_{HH} = 6.7$ Hz), 2.17 (s, 12H; $N(CH_3)_2$), 2.21 (s; 3H; NCH_3), 2.32 (t, 4H; CH_2, $^3J_{HH} = 7.0$ Hz), 2.44 (t, 4H; CH_2, $^3J_{HH} = 7.0$ Hz), 3.50 (h, 4H; CH, ^{i}Pr, $^3J_{HH} = 6.7$ Hz), 6.76–7.26 (m, 6H; ArH), 7.35 (br s, 1H; NC(H)N); $^{13}C\{^1H\}$ NMR (d_8-THF, 300 K): δ 24.7 (s; CH_3, ^{i}Pr), 28.8 (s; CH, ^{i}Pr), 33.6 (s; NCH_3), 46.5 (s; $N(CH_3)_2$), 57.7 (s; CH_2), 59.1 (s; CH_2), 123.5 (s; ArCH), 126.3 (s; ArC), 129.2 (s; ArC), 129.9 (s; ArCH), 143.8 (s; NCN).

5. X-ray crystallography

Crystalline samples of compounds **1**(THF), **1** · tol, **2**, **4**, **6** · tol, **7** and **8** were mounted in viscous hydrocarbon oil on glass fibres at −150 °C (123 K). Crystal data were obtained using an Enraf-Nonius Kappa CCD diffractometer. X-ray data were processed using the DENZO program [23]. Structural solution and refinement was carried out using the SHELX suite of programs [24,25] with the graphical interface X-Seed [26]. All hydrogen atoms were placed in calculated positions using the riding model. Crystal data and refinement parameters are compiled in Tables 1 and 2 with selected bond lengths and angles provided in Tables 3 and 4 (see reference key).

5.1. Variata

For compound **1** · tol, modelling of disorder for two ethyl CH_3 groups was attempted. This was successful for one (C(31)) but failed to give satisfactory thermal parameters for the other (C(8)). The disorder of C(31) was modelled over two sites of partial occupancy (59:41%) and C(8) was left as is.

For compound **2**, an ISOR refinement (0.01) was necessary to obtain satisfactory thermal parameters for C(11) and C(44). Modelling of disorder over two sites of partial occupancy for one THF methylene (C(87)) was attempted but failed to give satisfactory thermal parameters.

For compound **4**, modelling of disorder for a DME oxygen (O(3)) and two methylene groups (C(57) and C(58)) was attempted. This was successful for both carbon atoms but failed to give satisfactory thermal parameters for the O(3). The disorders of C(57) and C(58) were modelled over two sites of partial occupancy (A and B; 55:45% respectively) and O(3) was left as is.

For compound **6** · tol, data were poor. Disorder of the lattice toluene methyl group (C(58)) was modelled over two sites with 69:31% occupancy. Similarly, disorder of one ethyl CH_3 group (C(39)) and two PMDETA CH_3 groups ($N(CH_3)_2$; C(50) and C(51)) was modelled over two sites with 53:47% and 58:42% occupancy respectively. Further disorder, as suggested by prolate thermal parameters, could not be modelled successfully.

Data were poor for compound **8**. Attempts to model disorder suggested by prolate atomic thermal parameters were unsuccessful.

Acknowledgement

The authors would like to thank the Australian Research Council (ARC) for financial support and the EPRSC (UK) for a studentship (A.J.D.).

Appendix A. Supplementary material

CCDC 624458, 624459, 624460, 624462, 624463, 624464 and 624465 contain the supplementary crystallographic data for this paper. These data can be obtained free of charge via http://www.ccdc.cam.ac.uk/conts/retrieving.html, or from the Cambridge Crystallographic Data Centre, 12 Union Road, Cambridge CB2 1EZ, UK; fax: (+44) 1223-336-033; or e-mail: deposit@ccdc.cam.ac.uk. Supplementary data associated with this article can be found, in the online version, at doi:10.1016/j.jorganchem. 2007.02.028.

References

[1] (a) M.L. Cole, P.C. Junk, Chem. Commun., (2007), doi:10.1039/b613984a;
(b) J. Barker, M. Kilner, Coord. Chem. Rev. 133 (1994) 219;
(c) P.J. Bailey, S. Pace, Coord. Chem. Rev. 214 (2001) 91.
[2] (a) M.L. Cole, P.C. Junk, New J. Chem. (2005) 135;
(b) M.L. Cole, G.B. Deacon, C.M. Forsyth, P.C. Junk, K. Konstas, Dalton Trans. (2006) 3360.
[3] (a) M.L. Cole, G.B. Deacon, P.C. Junk, K. Konstas, Chem. Commun. (2005) 1581;
(b) M.L. Cole, P.C. Junk, Chem. Commun. (2005) 2695;
(c) M.L. Cole, G.B. Deacon, C.M. Forsyth, P.C. Junk, K. Konstas, J. Wang, Chem. Eur. J., in preparation.
[4] (a) R.J. Baker, C. Jones, P.C. Junk, M. Kloth, Angew. Chem., Int. Ed. Engl. 43 (2004) 3852;
(b) M.L. Cole, C. Jones, P.C. Junk, M. Kloth, A. Stasch, Chem. Eur. J. 11 (2005) 4482;
(c) C. Jones, P.C. Junk, J.A. Platts, D. Rathmann, A. Stasch, Dalton Trans. (2005) 2497;
(d) C. Jones, P.C. Junk, J.A. Platts, A. Stasch, J. Am. Chem. Soc. 126 (2006) 2206.
[5] M.L. Cole, D.J. Evans, P.C. Junk, M.K. Smith, Chem. Eur. J. 9 (2003) 415.
[6] Nomenclature used to describe amidinate isomers/tautomers is that described in S. Patai, Z. Rappoport (Eds.), The Chemistry of Amidines and Imidates, Wiley, Chichester, UK, 1991.
[7] J. Baldamus, C. Berghof, M.L. Cole, D.J. Evans, E. Hey-Hawkins, P.C. Junk, J. Chem. Soc., Dalton Trans. (2002) 2802.
[8] (a) Approximate pK_a values obtained from (a) HMDS; P. Rennaud, M.-A. Fox, J. Am. Chem. Soc. 110 (1988) 5702, and references cited therein;
(b) H_2 and ^{n}butane; M.B. Smith, J. March, Advanced Organic Chemistry, fifth ed., Wiley, Germany, 2000.
[9] J. Baldamus, C. Berghof, M.L. Cole, D.J. Evans, E.-M. Hey-Hawkins, P.C. Junk, J. Chem. Soc., Dalton Trans. (2002) 4185.
[10] E. Fluck, K.G. Heumann, Periodic Table of the Elements, VCH, Weinheim, Germany, 1991.
[11] M.L. Cole, P.C. Junk, J. Organomet. Chem. 666 (2003) 55.
[12] M.L. Cole, A.J. Davies, C. Jones, P.C. Junk, J. Organomet. Chem. 689 (2004) 3093.
[13] R.T. Boere, M.L. Cole, P.C. Junk, J.D. Masuda, G. Wolmerhauser, Chem. Commun. (2004) 2564.
[14] R.T. Boere, M.L. Cole, P.C. Junk, E.G. Robertson, unpublished material.
[15] (a) X.-W. Li, Y. Xie, P.R. Schreiner, K.D. Gripper, R.C. Crittendon, C.F. Campana, H.F. Schaefer, G.H. Robinson, Organometallics 15 (1996) 3798;
(b) X.-W. Li, W.T. Pennington, G.H. Robinson, J. Am. Chem. Soc. 117 (1995) 7578;
(c) B. Twamley, P.P. Power, Angew. Chem., Int. Ed. 39 (2000) 3500.
[16] D.B. Collum, Acc. Chem. Res. 25 (1992) 448.
[17] (a) M.A. Nichols, P.G. Williard, J. Am. Chem. Soc. 15 (1993) 1568;
(b) I. Keresztes, P.G. Williard, J. Am. Chem. Soc. 122 (2000) 10228.
[18] D. Seebach, R. Hassig, J. Gabriel, Helv. Chim. Acta 66 (1983) 308.
[19] (a) B. Qu, D.B. Collum, J. Am. Chem. Soc. 127 (2005) 10820;
(b) B. Qu, D.B. Collum, J. Am. Chem. Soc. 128 (2006) 9355.
[20] (a) M.F. Lappert, P.P. Power, A.R. Sanger, R.C. Srivastava, Metal and Metalloid Amides, Ellis Horwood Ltd, Chichester, England, 1980;
(b) A.M. Sapsa, P.v. R. Schelyer (Eds.), Lithium Chemistry: A Theoretical and Experimental Overview, Wiley Interscience, New York, USA, 1995;
(c) B.J. Wakefield, Organolithium Methods, Academic Press, New York, USA, 1988.
[21] Full data for compound **3** has been submitted to the Cambridge Crystallographic Data Centre as Supplementary information with submission number CCDC 624461. Unit cell parameters (Å and °); Monoclinic, $P2_1/c$; a 17.82130(10), b 23.0233(2), c 39.1519(4), β 93.3900(10), volume 16036.1(2) Å^3.
[22] R.M. Roberts, J. Org. Chem. 14 (1949) 277.
[23] Z. Otwinowski, W. Minor, Processing of X-ray diffraction data collected in oscillation mode, in: C.W. Cater, R.M. Sweet (Eds.), Macromolecular Crystallography, Part A, Methods in Enzymology, vol. 276, Academic Press, 1997, p. 307.
[24] G.M. Sheldrick, SHELXL-97, University of Göttingen, Germany, 1997.
[25] G.M. Sheldrick, SHELXS-97, University of Göttingen, Germany, 1997.
[26] L.J. Barbour, J. Supramol. Chem. 1 (2001) 189.